Electron dynamics in capacitively coupled RF discharges

J. Schulze[1], B.G. Heil, D. Luggenhölscher[1], T. Kampschulte[2], U. Czarnetzki[1]

[1] *Institute for experimental physics V, Ruhr-University Bochum (Germany) E-mail: fjschulze@hotmail.com*
[2] *Institute for Applied Physics, University Bonn (Germany)*

A laser spectroscopic method for sensitive electric field measurements using krypton has been developed. In a strongly asymmetric capacitively coupled radio-frequency discharge electric fields in the sheath were measured phase and space resolved within one RF-cycle. The excitation caused by beam like high energetic electrons, which are accelerated at the sheath edge, is measured by phase resolved optical emission spectroscopy (PROES). The plasma itself is characterised by langmuir probe measurements in terms of electron density, electron temperature and electron energy distribution function (EEDF). In parallel the RF voltage and the current to the chamber wall are measured. The synergistic effect of these diagnostics yields information on cause and effect of electron heating and a better understanding of these fundamental phenomena.

1. Introduction

Despite its technological importance, the complexity of power coupling mechanisms in capacitively coupled radio-frequency (CCRF) discharges is not yet fully understood. In particular, there is a lack of experimental investigations with regard to heating and excitation phenomena in these discharges.

In order to obtain a closer insight into these fundamental processes, one needs to investigate cause and effect of electron heating in CCRF discharges. The cause of electron heating is the electric field and its temporal as well as spatial evolution within one RF-cycle. Its effect is the time and space dependent ionisation in the plasma, which can be probed through excitation. Insight into power dissipation requires temporal resolution on a nanosecond time scale within the RF cycle for the investigation of the electric fields as well as the excitation dynamics.

The electric fields within the sheath are investigated by fluorescence dip spectroscopy (FDS) [1,2]. Here the technique is applied to krypton as a probe gas [3]. Knowledge of the field allows the determination of e.g. voltages, charge densities and currents.

The excitation dynamics is investigated by phase resolved optical emission spectroscopy (PROES). Both diagnostics are non-intrusive and provide high temporal and spatial resolution.

The plasma itself is characterised by radially resolved langmuir probe measurements in terms of electron density, electron temperature and electron energy distribution function (EEDF).

The current to the chamber wall as well as the RF voltage applied to the powered electrode are measured in parallel.

Space and phase resolved profiles of the electric field in the sheath and the excitation are presented and phenomena such as electron beams and plasma series resonances (PSR) are discussed based on the information from probe, current and voltage measurements. The synergistic effect of all these diagnostics can yield a complete picture of electron heating in CCRF discharges.

2. Experimental setup

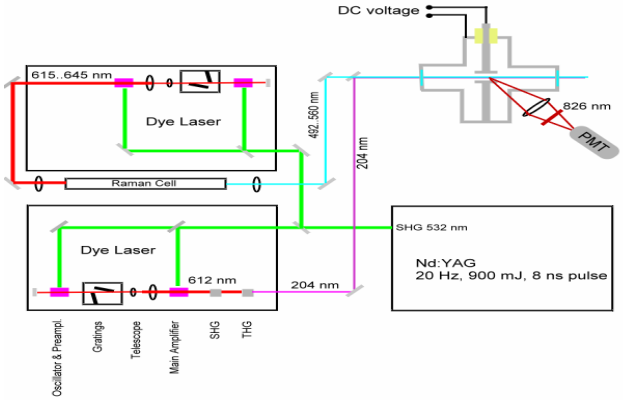

Fig. 1: Laser system and calibration cell

Figure 1 shows the experimental setup used for the investigation of the Stark effect in Krypton at known electric fields. The frequency-doubled output beam (532 nm) of a seeded Nd:YAG laser (Continuum, 9020) with a pulse width of 7 ns and pulse energy of 900 mJ at a repitition rate of 20 Hz pumps two tunable dye lasers (Radiant Dyes, Narrow Scan). The first dye laser beam is frequency-tripled for the needed two photon excitation step (204.13 nm, 3 mJ). The fundamental of the second dye laser is shifted into the desired wavelength intervall of 490 nm – 560 nm by the generation of the first Anti-Stokes within the Raman-effect in H_2. An electrical shutter switches the second laser beam on and off. Both beams are guided collinearly into the calibration cell. It contains two parallel plate capacitor-like electrodes (d = 9.8 mm) and is filled

with krypton at 0.3 Pa. Homogenous DC electric fields up to 3 kV/cm are provided without electrical breakdown. The fluorescence light is detected by a photomultiplier.

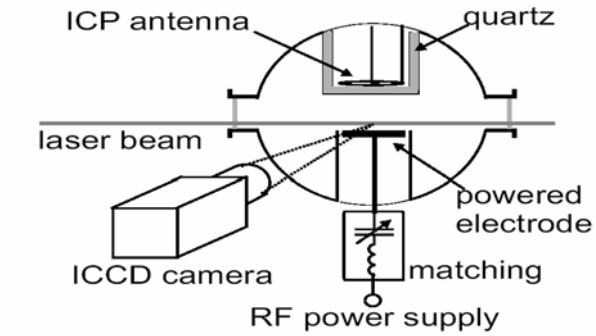

Fig. 2: GEC reference cell accessible for FDS and PROES

For the space and phase resolved measurements of electric fields in the sheath of a CCRF discharge the calibration cell is replaced by a modified GEC reference cell (figure 2). The discharge is strongly asymmetric, so that almost the entire voltage drops across the sheath at the powered electrode. The fluorescence light is observed with an ICCD camera, whose gate is synchronised with the laser pulse. The laser pulse is synchronised with the RF voltage. Therefore, phase resolved measurements of the electric field in the sheath are possible.
The Langmuir probe (Scientific Systems, Smart Probe) can be moved radially through the discharge 2.5 cm above the powered electrode.
The RF voltage is measured by a high voltage probe at the output of the matchbox, that is connected to the electrode. The current to the chamber wall is measured by a SEERS-sensor (ASI).

3. Results

3.1 Fluorescence Dip Spectroscopy in Krypton

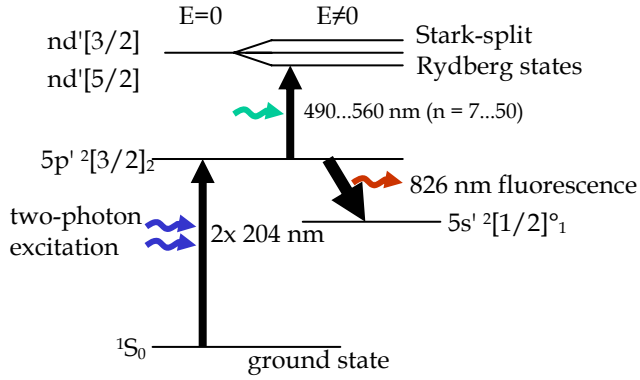

Fig. 3: Excitation scheme in krypton used for FDS

Figure 3 shows the excitation scheme used for FDS in krypton. It is based on TALIF spectroscopy, which has been used for measurements of neutral densities before [5]. Electrons are excited from the ground state by two-photon excitation (204.13 nm) into the intermediate level $5p'[3/2]_2$. Fluorescence to $5s'[1/2]_1$ at 826.3 nm is detected. The second dye laser excites electrons from the intermediate state to the Rydberg states, that are sensitive to electric fields. A certain wavelength interval is scanned with the second dye laser. If a transition into a Rydberg state is hit, the fluorescence decreases and a dip can be observed at a certain wavelength. If the electric field is known (calibration cell), a map of the Stark splitting of the Rydberg states of krypton can be produced, that can later be used for electric field measurements in the sheath of a CCRF discharge, where the fields are unknown.

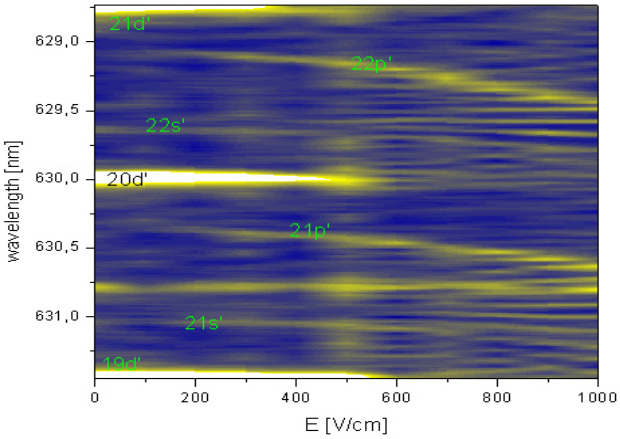

Fig. 4: Measured Stark map in krypton in the range 19*d*-21*d*. The fluorescence decrease is indicated by bright lines

Figure 4 shows the result of this calibration for a wavelength interval between 19d' and 21d'. One can clearly identify the quadratic Stark shift of different ns', nd' and np' levels as well as the linear Stark shift of nl' levels [3]. The line shifts were also calculated theoretically showing good agreement with the measured Stark map [3].

3.2 Space and phase resolved electric fields and excitation dynamics in a CCRF discharge

Using the database of Stark shifts of various Rydberg states of krypton, electric fields in the sheath of a CCRF discharge can be measured spatially and temporally resolved. Figure 5 shows an exemplary result of such a measurement in a krypton discharge at 1 Pa and 8 W. One can observe the sheath expansion and collapse as well as an asymmetry between these two phases in terms of the spatial distribution of the electric field.
Under the same conditions the space and phase resolved excitation into $Kr2p_5$ can be measured. As the excitation threshold of this line is 11.7 eV,

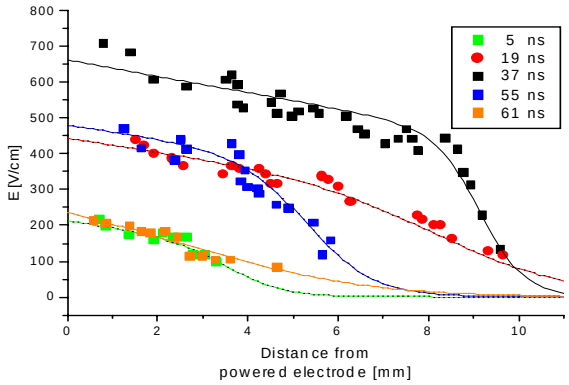

Fig. 5: Space and phase resolved electric fields in a strongly asymmetric CCRF discharge (Kr, 1 Pa, 8 W)

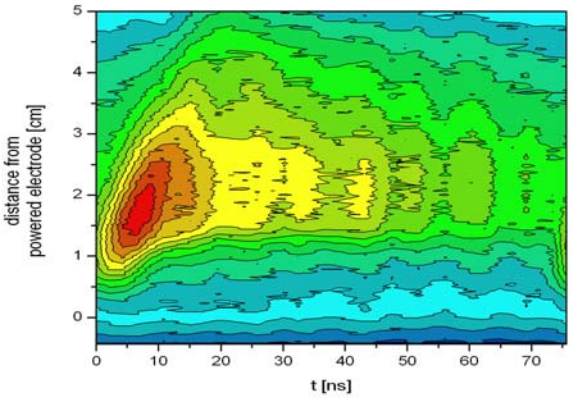

Fig. 6: Space and phase resolved excitation into $Kr2p_5$ in a krypton discharge at 1 Pa and 8 W (gatewidth 4.2 ns)

$Kr2p_5$ is only sensitive to high energetic electrons. An absolute phase calibration between both diagnostics has been performed, so that the time scales in figures 5 and 6 are the same. During the sheath expansion phase (5-19 ns, figure 5) electrons are strongly accelerated by the moving sheath edge and an electron beam is launched, that penetrates into the bulk (figure 6). Later modulations of the excitation at the sheath edge can be attributed to the PSR effect [6]. The maximum sheath width is 1 cm both in the electric field as well as the excitation measurements.

Figure 7 shows a comparison between the measured RF voltage and the voltage, that results from an integration of the measured electric fields (figure 5) at different phases. The good agreement demonstrates the applicability of FDS in krypton. Figure 7 also shows the dependence of the sheath voltage U_s on the square of the surface charge density σ. This proportionality is a fundamental assumption in terms of an analytical description of the PSR-effect [7]. It results from the assumption of a quasi-static ion density in the sheath and a step-function for the electron density.

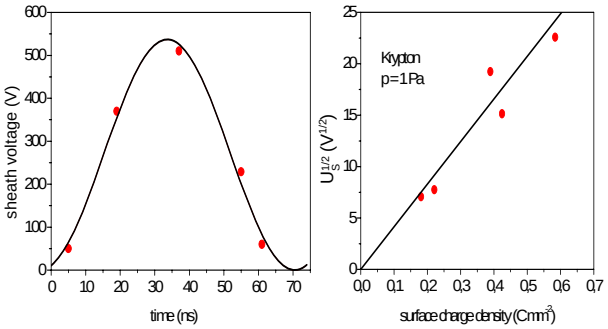

Fig. 7: Comparison between measured (high-voltage probe) and calculated sheath voltages (E-fields) and sheath voltage vs. surface charge density

Analogue investigations were performed at higher pressures. The plasma itself is characterised by langmuir probe measurements in terms of electron density, -temperature and EEDF.

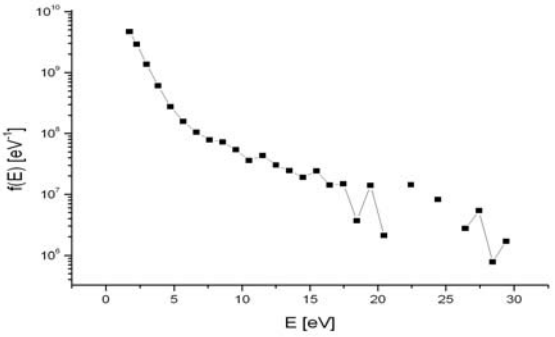

Fig. 8: EEDF obtained from langmuir probe measurements 2,5 cm above the powered electrode in pure Kr at 10 Pa and 8 W

Figure 8 shows an exemplary EEDF obtained from a probe measurement 2,5 cm above the powered electrode in pure Kr at 10 Pa and 8 W. The shape of the EEDF is bi-Maxwellian showing two different temperatures for the low and high energetic part of the distribution function. This shape is typical for CCRF discharges at low pressures.

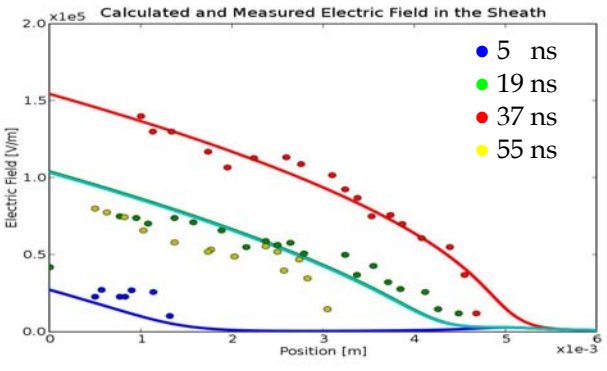

Fig. 9: Comparison between measured (points) and calculated (lines) electric fields (Kr, 10 Pa, 8 W)

The results of the probe measurements (electron density and –temperature) in combination with the measured RF-voltages were used as input parameters of a fluid sheath model of Brinkmann [8], that calculates the electric fields theoretically spatially and temporally resolved. A comparison between measured and calculated electric fields at different phases (10 Pa, 8 W) is shown in figure 9.

3.3 Electron beams and Plasma Series Resonance

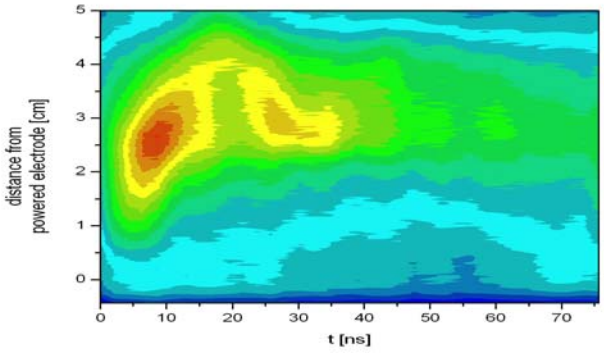

Fig. 10: Space and phase resolved excitation into $Ne2p_1$ in a neon discharge at 2 Pa and 8 W

Figure 10 shows a spatio-temporal plot of the excitation into $Ne2p_1$ in pure Ne at 2 Pa and 8 W. During the sheath expansion phase a beam of high energetic electrons is generated, that penetrates into the plasma bulk and is reflected at the plasma wall and the bottom electrode sheath. The lower the pressure, the larger the electron mean free path and the more reflections can be observed.

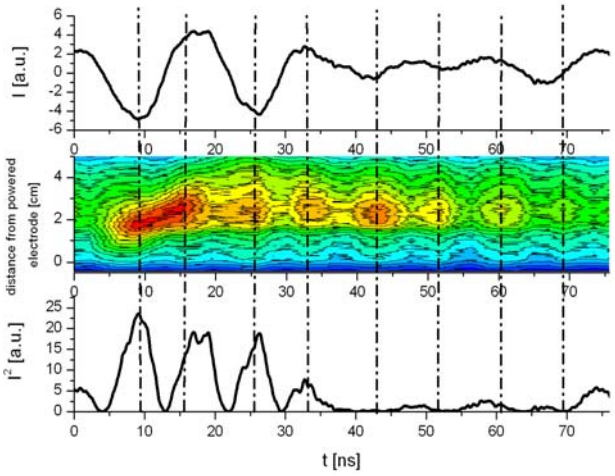

Fig. 11: Space and phase resolved excitation into $Kr2p_5$ and current in a krypton discharge at 0.5 Pa and 8 W

At extremely low pressures (< 2 Pa) the plasma series resonance effect [6] can be observed in terms of high frequency oscillations of the current and excitation at the sheath edge. At 0,5 Pa and 8 W figure 11 shows the generation of an electron beam during the sheath expansion phase and high frequency oscillations of the excitation during the entire RF-cycle. The correlation with the current to the chamber wall is also shown. Similar modulations of the excitation have also been observed in H_2 [9].

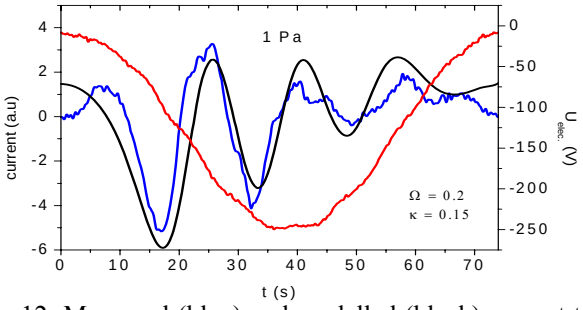

Fig. 12: Measured (blue) and modelled (black) current to the chamber wall and RF-voltage in Kr at 1 Pa and 8 W.

Figure 12 shows current and voltage measurements at 1 Pa and 8 W. In contrast to higher pressures and usual assumptions the current is not sinusoidal, but strong high frequency modulations similar to the modulations of the excitation can be observed. Measurements are in good agreement with theoretical calculations applying an analytical PSR model of Czarnetzki and Brinkmann [7].

4. Conclusions

Cause and effect of electron heating in CCRF discharges have been studied using the synergistic effect of various diagnostics. FDS in krypton was applied for the first time in order to measure electric fields in the sheath at high spatial and temporal resolution. The results show good agreement with simulations and spatio-temporal plots of the excitation (PROES).

The generation of beams of high energetic electrons by the expanding sheath and their reflections at the plasma boundaries could be observed by PROES.

At extremely low pressures (< 2 Pa) the PSR effect was observed both in terms of the excitation and current to the chamber wall. Comparisons to an analytical PSR model show good agreement.

5. Acknowledgement

The project is funded by the SFB 591 and GK 1051.

6. References

[1] Czarnetzki et al. *Phys. Rev. Lett.* **81** (1998) 4592
[2] Czarnetzki et al. *Plas. Sourc.* **8** (1999) 230-248
[3] Kampschulte et. al. *New J. Phys.* **9** (2007) 18
[5] Niemi *PhD thesis* (2003) Cuvillier Verlag
[6] Mussenbrock et. al. *APL.*(2006) **88** 151503
[7] Czarnetzki et al. *Phys. Plas.* **13** (2006) 123503
[8] Kratzer et al. J. Appl. Phys. **90** (2001) 2169
[9] O'Connell et. al. *Phys. Plas.* **14** (2007) 034505